Colloid Polym Sci (2009) 287:577–582
DOI 10.1007/s00396-009-2005-4

ORIGINAL CONTRIBUTION

Synthesis of amphiphilic polysiloxanes and their properties for formation of nano-aggregates

Norio Iwakiri · Takehiro Nishikawa · Yoshiro Kaneko · Jun-Ichi Kadokawa

Received: 06 November 2008 / Revised: 12 January 2009 / Accepted: 14 January 2009 / Published online: 13 February 2009

Abstract In this study, we prepared amphiphilic polysiloxanes by introduction of hydrophobic and hydrophilic parts into a water-soluble poly(3-aminopropyl)siloxane. Fatty acid (lauroyl, myristoyl, palmitoyl, and stearoyl) chlorides and gluconolactone were employed as the reactants for the hydrophobic and hydrophilic parts, respectively. The reaction of the poly(3-aminopropyl)siloxane with fatty acid chlorides was performed in water/DMF, followed by the reaction with gluconolactone in DMSO, giving the corresponding amphiphilic polysiloxanes. The results of the NMR spectra, SEM observations, and DLS measurements indicated the formation of nano-aggregates from the amphiphilic polysiloxanes in water. These analytical data also suggested that the structures and functionalities of the hydrophobic parts affected the formation properties of the nano-aggregates.

Keywords Polysiloxane · Amphiphilic · Fatty acid · Gluconolactone · Nano-aggregate

Introduction

Silicon derivatives are known to be attractive materials because they exhibit low toxicity and specific physical properties. Therefore, they have been widely used as versatile products such as foam stabilizer, rubber, paint, fiber, glass, and textile [1]. Silicon-containing polymers such as polydimethylsiloxane also have various interesting properties, e.g., hemocompatibility, biocompatibility, and anti-inflammatory properties, which would be advantages as biomaterials [2]. However, the polysiloxane-based materials have not been studied on their ability for the formation of nano-aggregates as biomaterials such as the carrier for drug delivery systems. To obtain the nano-aggregates or nano-particles from the polymeric materials, the amphiphilic nature has been known to contribute to the property for their self-aggregation in aqueous solution [3]. In the previous study, we paid attention to an amine-functionalized polysiloxane **1** as the starting material for the preparation of the nano-aggregates from the silicon-containing polymeric material [4]. The polysiloxane **1** was prepared by sol–gel reaction of amine-substituted organoalkylsilanes in strong acid aqueous solution [5]. The material was soluble in water and had reactive amino groups on the surface, which were considered to be the favorable nature and structure for the introduction of functional groups in the polysiloxane main chain by reaction with appropriate reactants.

In our previous paper, the synthesis of the amphiphilic polysiloxanes having the stearoyl chains and the sugar residues as hydrophobic and hydrophilic parts, respectively, was performed by the successive reactions of **1** with stearoyl chloride and with lactobionolactone under appropriate conditions [6]. We also briefly showed that the amphiphilic polysiloxane with the functionalities of 2% and 48% for the hydrophobic and hydrophilic parts, respectively, formed the particle-type nano-aggregates with several tens of nanometers in water. We have been studying cellular uptake of the nano-particles from the amphiphilic polysiloxanes in human aortic endothelial cells on the basis of

N. Iwakiri · Y. Kaneko · J.-I. Kadokawa (✉)
Department of Nanostructured and Advanced Materials,
Graduate School of Science and Engineering,
Kagoshima University,
1-21-40 Korimoto,
Kagoshima 890-0065, Japan
e-mail: kadokawa@eng.kagoshima-u.ac.jp

T. Nishikawa
National Cardiovascular Center Research Institute,
5-7-1 Fujishirodai,
Suita, Osaka 565-8565, Japan

the following idea, in which the induction of nitric oxide (NO) release synthesized by endothelial nitric oxide synthase (eNOS) is possibly caused by the delivery of the nano-particles to endothelial cells. This investigation has been a first attempt for the potential and novel medication to hypertension on the basis of the regulation of NO release by switching of eNOS activation in a single cell affected by targeting delivery of nano-particles. Because it has been pointed out that caveolae, micro domains in the plasma membrane of a cell, are the important pathways for drug delivery at endothelium [7], the shape, size, and size distribution of the nano-particles may affect internalization of external substances and cell signallings leading to NO release. However, the property for the formation of the amphiphilic polysiloxane particles and the control of their shapes, sizes, and size distributions have not been established well, which are probably affected by structure and functionality of the hydrophobic and hydrophilic parts.

On the basis of the above viewpoints, in this paper, we report the synthesis of the amphiphilic polysiloxanes having the various structures of the hydrophobic parts derived from the fatty acids, combined with a hydrophilic part (Scheme 1). For the introduction of the hydrophilic part, we herein took up the reaction with gluconolactone, which is a more widely used and simplified sugar lactone compared with lactobionolactone employed in our previous study [6]. The property for the formation of the nano-aggregates from the synthesized amphiphilic polysiloxanes in water in terms of the structures of the hydrophobic parts was evaluated using ^{1}H NMR, scanning electron microscopy (SEM), and dynamic light scattering (DLS) analyses. Furthermore, the relation of the functionality of the hydrophobic part to the property for the formation of the aggregates was also revealed.

Experimental

Materials and methods

The polysiloxane **1** was prepared according to the literature procedure [5]. Other reagents and solvents were used as received. The ^{1}H NMR spectra were recorded on a JEOL ECX400 spectrometer. The SEM images were obtained using a Hitachi S-4100 electron microscope. The average particle diameters and standard deviations were calculated on the basis of 100 objects or more for each SEM image. The DLS measurement was performed on a Zetasizer 3000

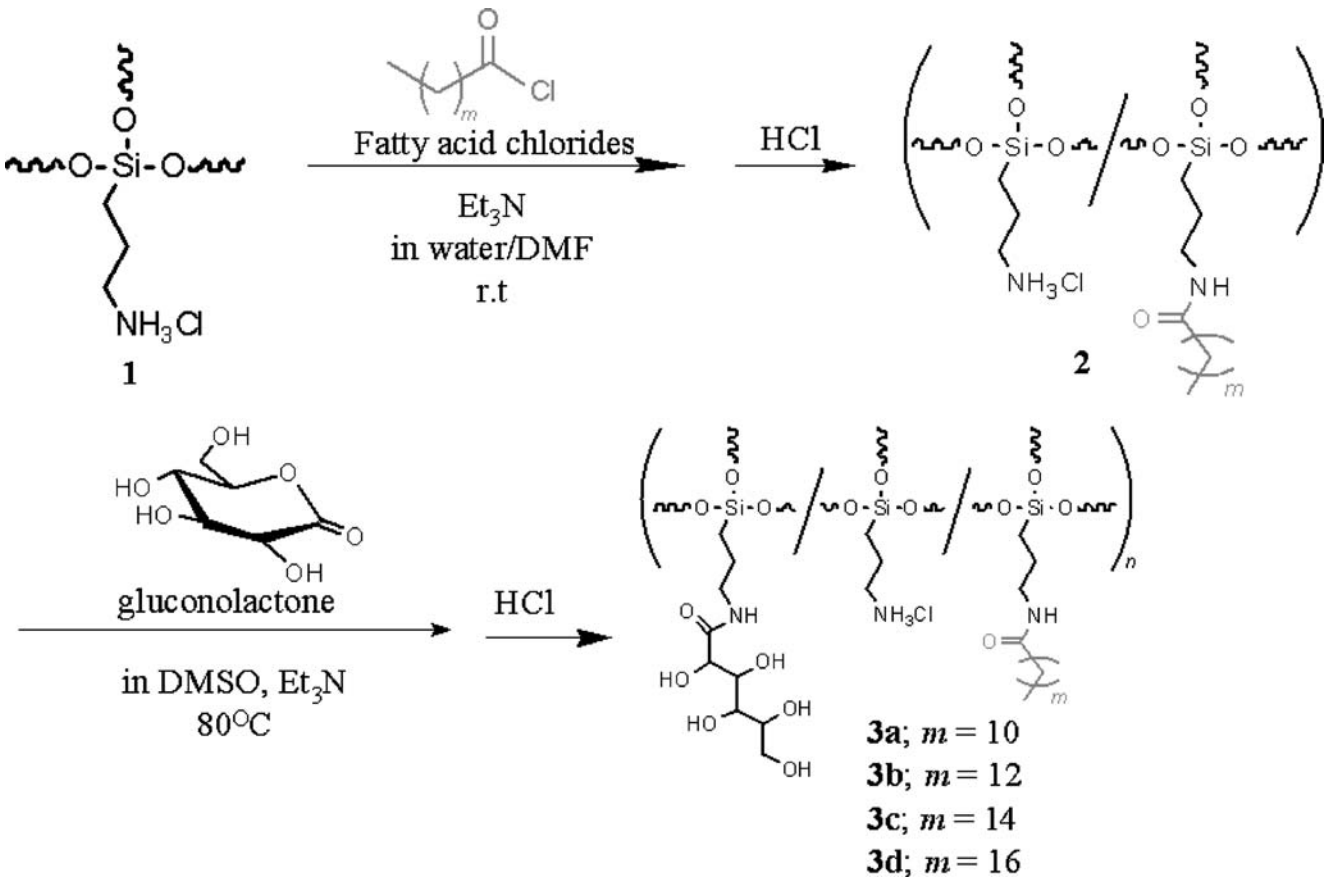

Scheme 1 Preparation of amphiphilic polysiloxanes **3a**–**d**

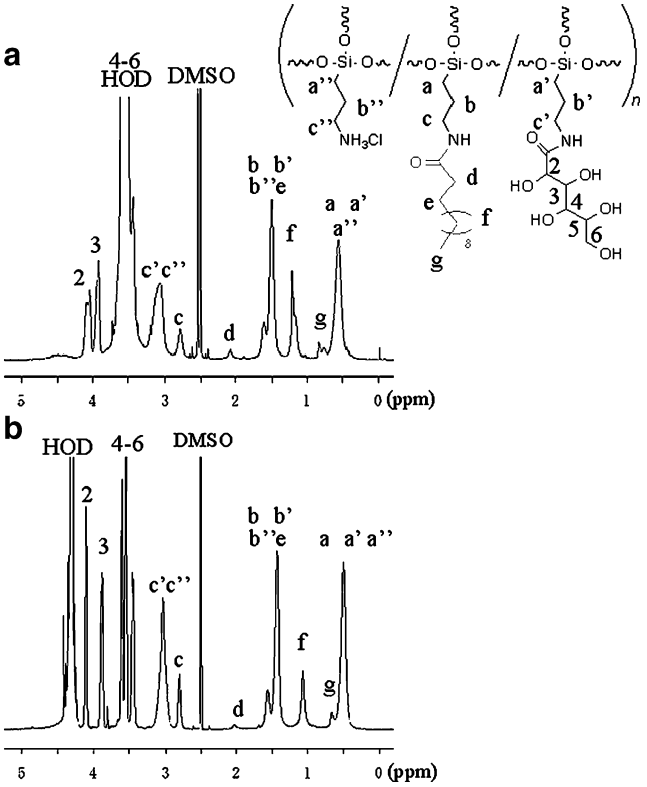

Fig. 1 ^{1}H NMR spectra of **3a** measured in DMSO-d_6 (containing a small amount of D_2O) (**a**) and D_2O (**b**)

(Malvern Instruments). DLS measures the intensity of light scattered by the sample. Intensity fluctuation of the scattered light is computationally processed and converted to an autocorrelation function. Autocorrelation function represents the intensity fluctuation in time. The autocorrelation function in DLS is represented by the following equation; $g_2(t)=Ae^{-2\Gamma t}+1$, where $g_2(t)$ is the autocorrelation function, A is an amplitude factor, Γ is the decay rate, and t is the time-shift. The intensity fluctuation is caused by Brownian motion of particles in solution. Therefore, the decay rate, Γ, in the autocorrelation function is related to the diffusion coefficient, D_t, of the particles; $\Gamma=D_tq^2$, where q is scattering vector and defined by the following equation; $q=(4\pi n/\lambda)\sin(\phi/2)$ where λ is laser wavelength, n is refractive index, and ϕ is scattering angle. D_t is calculated by fitting the autocorrelation function to an exponential function. Hydrodynamic radius (R_h) of particles is related to D_t in the Stokes–Einstein equation; $D_t=KT/6\pi\eta R_h$, where K is Boltzman's constant, T is absolute temperature, and η is solvent viscosity. R_h is calculated from D_t using data processing software attached to the DLS apparatus (DTS Nano Ver. 5.0).

Synthesis of amphiphilic polysiloxanes

A typical experimental procedure was as follows (synthesis of **3a**): To a solution of **1** (0.441 g, 4.00 mmol) in water (10.0 mL), triethylamine (1.30 mL, 9.60 mmol) and a solution of lauroyl chloride (0.219 g, 1.00 mmol) in DMF (30.0 mL) were rapidly added in this order and the mixture was stirred at room temperature for 10 min. After 5.0 mol/L hydrochloric acid (3.84 mL, 19.2 mmol) was added to the reaction mixture and stirred for 5 min, the solution was poured into acetone (500 mL) to precipitate the product. The precipitate was isolated by filtration, washed with chloroform and acetone, and dried under reduced pressure to give **2** (0.4294 g). The obtained product (0.349 g, 2.90 mmol) was dissolved in DMSO (7.0 mL) and, to this solution, triethylamine (1.00 mL, 7.40 mmol) and a solution of gluconolactone (2.58 g, 14.5 mmol) in DMSO (13.0 mL) were added in this order. After the mixture was stirred at 80 °C for 2 h, the resulting solution was poured into ethanol (500 mL) to precipitate the product. The precipitate was isolated by filtration, washed successively with HCl methanol, methanol, and ethanol, and dried under

Table 1 Preparation, ^{1}H NMR analysis, SEM and DLS results of amphiphilic polysiloxanes

Sample	Number of carbon in hydrophobic part	Functionality (%)[a]		Decreasing ratio of a signal due to hydrophobic part in ^{1}H NMR spectrum (%)[b]	SEM result		DLS result in water	
		Hydrophobic	Hydrophilic		Average diameter (nm)	Standard deviation	Z-average diameter (nm)	PDI
3a	12	5.3	88.8	31.8	74.7	22.1	74.9	0.23
3b	14	5.3	88.8	19.0	54.6	25.8	52.3	0.38
3c	16	4.5	91.4	26.8	61.6	28.4	62.2	0.44
3d	18	4.9	92.4	21.6	71.7	23.9	51.7	0.38
3a-1	12	1.8	84.0	22.2	107.8	21.6	37.8	0.52
3a-4	12	4.6	86.2	27.9	70.1	23.7	61.7	0.42
3a-6	12	6.3	82.7	37.0	60.0	17.2	78.5	0.24
3a-8	12	8.1	81.7	20.0	62.1	16.2	87.6	0.15

PDI; polydispersity index

[a] Determined by ^{1}H NMR spectrum in DMSO-d_6 (containing a small amount of D_2O)

[b] Comparison in ^{1}H NMR spectra measured in DMSO-d_6 (containing a small amount of D_2O) and in D_2O

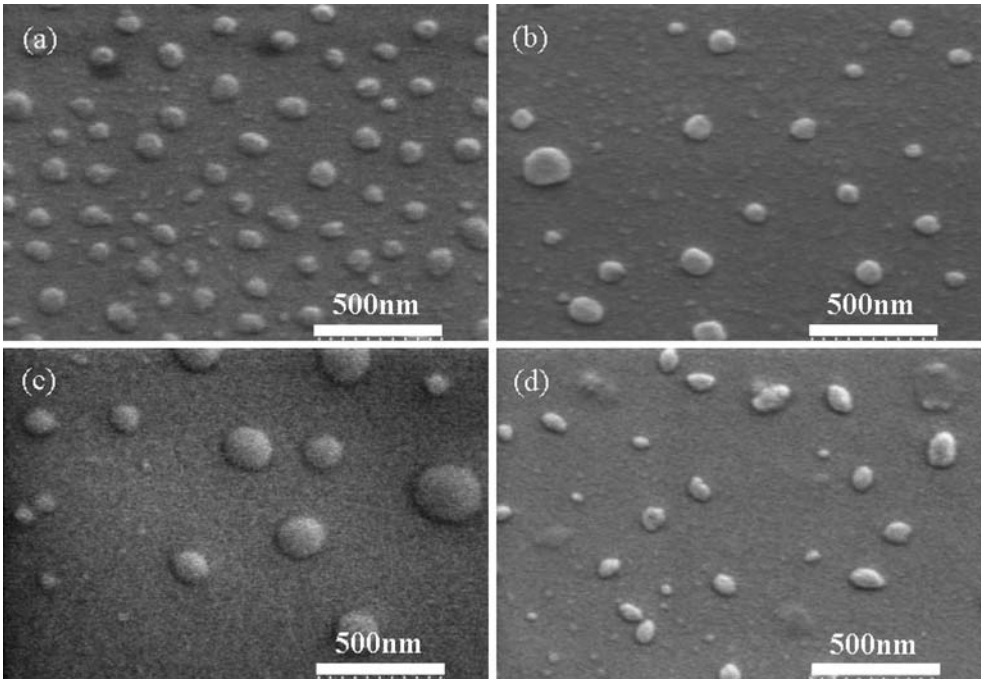

Fig. 2 SEM images of **3a** (**a**), **3b** (**b**), **3c** (**c**), and **3d** (**d**)

reduced pressure to obtain the crude material (0.499 g). The product (0.0307 g, 0.110 mmol) was suspended in water (5.0 mL) and the suspension was filtered through the membrane filter with the pore size of 2 μm. The filtrate was lyophilized to give **3a** (0.0249 g). ^{1}H NMR (DMSO-d_6 containing a small amount of D_2O): δ 0.35–0.88 (br, CH_3, CH_2—Si), 1.09–1.29 (br, C—(CH_2)$_9$—CH_3), 1.34–1.79 (br, CH_2—C—Si, CH_2—C—C═O), 1.99–2.12 (br, CH_2—C═O), 2.71–3.27 (br, CH_2—N), 3.32–3.74 (br, C*H*(OH)C*H*(OH)CH_2), 3.85–3.99 (br, C*H*CH(OH)C═O), 3.99–4.18 (br, CHC═O).

The amphiphilic polysiloxanes **3b**–**d** were prepared by the same procedure as described above using myristoyl, palmitoyl, and stearoyl chlorides, respectively.

Results and discussion

As previously reported by us [6], the amphiphilic polysiloxanes have been prepared by the reaction of **1** with fatty acid chloride in water/DMF, followed by the reaction with sugar lactone in DMSO. In this study, we synthesized four amphiphilic polysiloxanes **3a**–**d** having the hydrophobic parts with different alkyl chain lengths (C_{12}–C_{18}) accompanied with the hydrophilic part derived from gluconolactone according to Scheme 1. The functionalities of the hydrophobic and hydrophilic parts in **3a**–**d** were adjusted to ca. 5% and 90 %, respectively, by controlling the ratios of **1**, fatty acid chlorides, to gluconolactone in feeds. The crude materials obtained by the two reaction steps were suspended in water and the suspensions were filtered through the membrane filter with the pore size of 2 μm. Then, the filtrates were lyophilized to give the products **3a**–**d**, which were soluble in DMSO, and thus their structures were confirmed by the ^{1}H NMR spectra measured in DMSO-d_6 (containing a small amount of D_2O). Figure 1a shows the ^{1}H NMR spectrum of **3a** in DMSO-d_6 (containing a small amount of D_2O). All the signals were fully assignable to the structure of **3a** and the functionalities of the hydrophobic and hydrophilic parts were calculated by the integrated ratios of the signal **f**, the signals **a**, **a′**, and **a″**, to the signals **2** and **3** to be 5.3% and 88.8 %, respectively. Interestingly, the signal intensity of H**f** due to the lauroyl group measured in D_2O (Fig. 1b) was lower than that in DMSO-d_6 (Fig. 1a). This observation indicated that the lauroyl groups attached to polysiloxane backbone aggregated upon the intra- and intermolecular aggregation of **3a** in D_2O. In the ^{1}H NMR

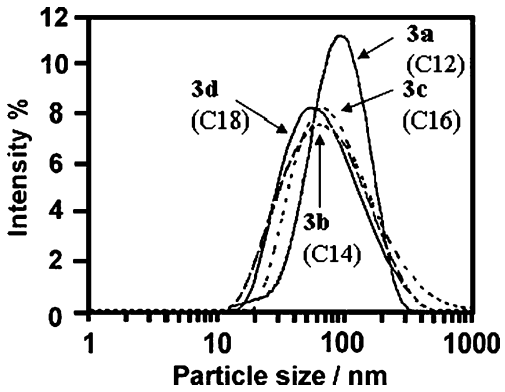

Fig. 3 DLS profiles of **3a**–**d** in water

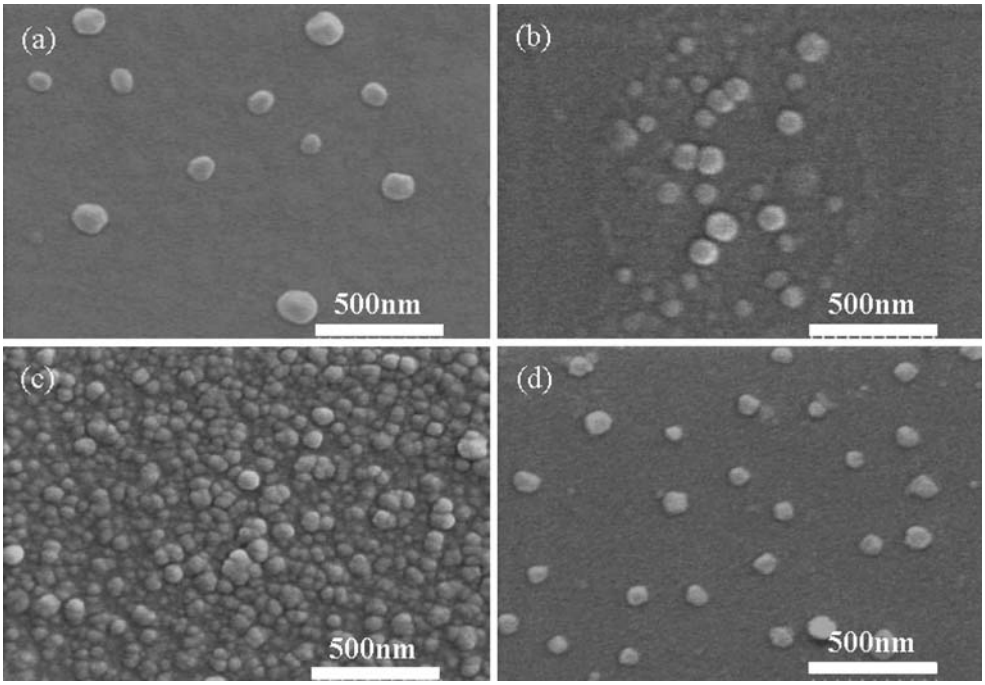

Fig. 4 SEM images of **3a-1** (**a**), **3a-4** (**b**), **3a-6** (**c**), and **3a-8** (**d**)

analyses of the other amphiphilic polysiloxanes **3b**–**d**, the similar phenomena were observed and the decrease in the signal intensity due to alkyl chains was estimated by the ratio of the signal intensity measured in D_2O to that in DMSO-d_6. These data listed in Table 1 indicated that the extent of decrease in the signal intensity of H**f** in **3a** was larger than that of **3b**–**d**, indicating that the lauroyl group was more favorable as the hydrophobic part in the amphiphilic polysiloxane for the formation of aggregates in water than the other alkanoyl groups.

To confirm the formation properties of the aggregates from **3a**–**d** in water in detail, the SEM and DLS measurements were conducted. Figure 2 shows the SEM images of the spin-coated samples on the glass plates from the aqueous solutions of **3a**–**d**. The average particle diameters and standard deviations were calculated on the basis of the lengths of the long and short axis, respectively, of 100 or more nanoparticles in each SEM image. These are listed in Table 1. The image from **3a** (Fig. 2a) indicates the formation of the particle-type nano-aggregates with the average diameter of 74.7 nm. Although the nano-particles are also observed in the images from **3b** and **c** (Fig. 2b, c), the values of the standard deviations for these SEM images (25.8 and 28.4, respectively) are larger than that for Fig. 2a (22.1). Moreover, the aggregates from **3d** in Fig. 2d do not exhibit the clear particle shape. The DLS measurements of the solutions of **3a**–**d** in water also revealed the narrower particle size distribution of the aggregates from **3a** (Fig. 3 and Table 1) than that from the other amphiphilic polysiloxanes. The difference in particle size between SEM and DLS is attributable to the sample conditions (wet or dry) in these measurements. These SEM and DLS results suggested that **3a** formed the nano-particles with the regulated shape and narrow size distribution compared with **3b**–**d**. This is probably due to the strong inter- or intramolecular interaction of the lauroyl groups in **3a**, which is in good agreement with the aforementioned NMR data. On the basis of the above results, it can be considered that the chain length of the hydrophobic parts does not affect significantly the average particle size but considerably influences the size distribution.

Because **3a** exhibited the suitable property for the formation of the nano-particles with the narrower size distribution in the four amphiphilic polysiloxanes **3a**–**d**, we then examined the effect of the functionality of the lauroyl group in **3a** on the formation of the nano-particles. For this purpose, we prepared four amphiphilic polysiloxanes having the lauroyl groups with the different functionalities

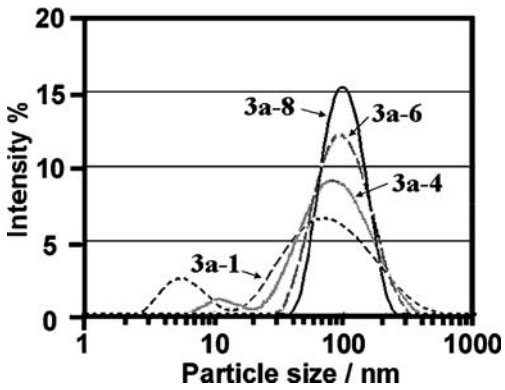

Fig. 5 DLS profiles of **3a-1**, **4**, **6**, and **8** in water

by changing the feed ratios of **1** to lauroyl chloride in the experiment of the functionalization. The functionalities were calculated by the ^{1}H NMR spectra of the products to be 1.8, 4.6, 6.3, and 8.1 with the similar functionalities of the hydrophilic part as ca. 90%. The amphiphilic polysiloxanes with different functionality of lauroyl group are now named as **3a-1**, **3a-4**, **3a-6**, and **3a-8**, respectively. The signal intensities due to the lauroyl group in all the ^{1}H NMR spectra of these four samples decreased by comparison to the signal intensity of the amphiphilic polysiloxane in DMSO-d_6 when ^{1}H NMR measurements were performed on the amphiphilic polysiloxanes dispersed in D_2O. Additionally, the reduction of the signal intensity in the ^{1}H NMR spectra of **3a-6** was largest of all the polysiloxane samples tested. These NMR results indicated that all the amphiphilic polysiloxanes with the different functionalities of the lauroyl group possibly formed the aggregates in water. Furthermore, **3a-6** was probably more favorable for the formation of the aggregates than others.

Then, the SEM and DLS measurements of these samples were performed to reveal the formation properties of the aggregates in water in detail. Figure 4 shows the SEM images of the spin-coated samples on the glass plates from the aqueous solutions of the four samples. A large number of the aggregates with the average diameter of 60.0 nm are observed in the image from **3a-6** (Fig. 4c), and the image from **3a-8** exhibits the aggregates with the average diameter of 62.1 nm and the smaller standard deviation value (Fig. 4d). Although the aggregates are also seen in the image from **3a-4** (average, 70.1 nm), the value of standard deviation (23.7) is obviously wider than that from **3a-6** and **3a-8** (17.2 and 16.2, respectively); the image looks like that in Fig. 3 because the functionalities of the hydrophobic and hydrophilic parts in both **3a** and **3a-4** are similar. The aggregates were difficult to be found in the image from **3a-1**, and even if we detected some aggregates their shapes were not good as shown in Fig. 4a. The SEM results suggested that **3a-6** was more favorable for the formation of aggregates in water, but the more regularly ordered nano-particles were obtained from **3a-8**, which were also supported by the following DLS data. The DLS results shown in Fig. 5 and Table 1 indicated that the particle size distribution of **3a-8** was narrower than that of the other samples, which was in good agreement with the SEM results. Furthermore, the DLS profile of **3a-1** exhibited a smaller mean diameter of ca. 5–6 nm, probably attributed to a single polysiloxane molecule besides a larger diameter of ca. 70 nm due to the aggregates. This DLS result in addition to the SEM result of the same sample (Fig. 4a) suggested that **3a-1** had the unfavorable nature for the formation of the aggregates in water, probably attributed to the less amphiphilic nature because of the less amounts of the hydrophobic parts in polysiloxane backbone. Because the average diameter in the DLS measurement was calculated on the basis of the aggregates with both the size regions, the value for **3a-1** (37.8 nm) was much smaller than that in the SEM measurement (107.8 nm). From the above SEM and DLS results, we concluded that the nano-particles with the narrower size distribution were formed by increasing the functionalities of the lauroyl groups although the sizes were not clearly affected by them.

Conclusion

The amphiphilic polysiloxanes were prepared by the reaction of the amine-functionalized polysiloxane **1** with fatty acid chlorides, followed by the reaction with gluconolactone. The ^{1}H NMR, SEM, and DLS analyses of the products suggested that the lauroyl group as the hydrophobic part was more suitable for the formation of the nano-particles with the regulated shape and narrow size distribution than myristoyl, palmitoyl, and stearoyl groups. Furthermore, the analytical results of the amphiphilic polysiloxanes having the lauroyl groups with the different functionalities revealed that the nano-particles with the narrower size distribution were formed by increasing the functionalities. Consequently, the present study concluded that the regularity of the nano-aggregates in water formed from the amphiphilic polysiloxanes was relatively controlled by the chain lengths and functionalities of the hydrophobic parts. We will investigate the effect of the shapes and size distributions of the amphiphilic polysiloxane particles on the cellular uptake in human aortic endothelial cells as well as the induction of NO release in a future study.

Acknowledgment T.N. thanks Dr. Tetsuji Yamaoka and Dr. Atsushi Mahara of the National Cardiovascular Center for DLS measurement.

References

1. Kichler A, Sabourault N, Décor R, Leborgne C, Schmutz M, Valleix A, Danos O, Wagner A, Mioskowski C (2003) J Control Release 93:403
2. Bélanger MC, Marois Y (2001) J Biomed Mater Res 5:467
3. Kwon GS (2003) Critical Reviews in Therapeutic Drug Carrier 20:357
4. Kaneko Y, Kadokawa J, Setoguchi M, Iyi N (2005) Polymer 46:8905
5. Kaneko Y, Iyi N, Kurashima K, Matsumoto T, Fujita T, Kitamura K (2004) Chem Mater 16:3417
6. Beppu K, Kaneko Y, Kadokawa J, Mori H, Nishikawa T (2007) Polym J 39:1065
7. Muro S, Koval M, Muzykantov V (2004) Curr Vasc Pharmacol 2:281